



## ORIGINAL ARTICLE

# Irinotecan-induced alterations in intestinal cell kinetics and extracellular matrix component expression in the dark agouti rat

Noor Al-Dasooqi<sup>\*,†</sup>, Joanne M. Bowen<sup>\*,†</sup>, Rachel J. Gibson<sup>†,‡</sup>, Richard M. Logan<sup>§,¶</sup>, Andrea M. Stringer<sup>†,‡</sup> and Dorothy M. Keefe<sup>\*,†,\*\*,§</sup>

<sup>\*</sup>Department of Medicine, University of Adelaide, North Terrace, Adelaide, SA, Australia, <sup>†</sup>Department of Medical Oncology, Royal Adelaide Hospital, North Terrace, Adelaide, SA, Australia, <sup>‡</sup>School of Medical Sciences, University of Adelaide, North Terrace, Adelaide, SA, Australia, <sup>§</sup>Division of Surgical Pathology, SA Pathology, Adelaide, SA, Australia, <sup>¶</sup>Oral Pathology, School of Dentistry, Faculty of Health Sciences, University of Adelaide, North Terrace, Adelaide, SA, Australia and <sup>\*\*</sup>Cancer Council South Australia, Eastwood, SA, Australia

## INTERNATIONAL JOURNAL OF EXPERIMENTAL PATHOLOGY

doi: 10.1111/j.1365-2613.2011.00771.x

Received for publication: 11  
November 2010  
Accepted for publication: 28 February  
2011

### Correspondence:

Noor Al-Dasooqi  
Royal Adelaide Hospital  
Department of Medical Oncology  
Level 4 East Wing  
North Terrace  
Adelaide, SA 5000  
Australia  
Tel.: +61 8 82223547  
Fax: +61 8 82223217  
E-mail: noor.al-dasooqi@  
adelaide.edu.au

## Summary

Chemotherapy-induced mucositis is characterized by damage of mucous membranes throughout the alimentary tract (AT). Extracellular matrix (ECM) components play a vital role in maintaining mucosal barrier integrity by regulating cellular apoptosis, proliferation and differentiation of overlying epithelial cells. The aims of this study were to characterize the changes in epithelial cell kinetics and to investigate the expression of the ECM components in the gastrointestinal tract following irinotecan administration. Female dark agouti rats were treated with single 200 mg/kg dose irinotecan and killed at various time points (1, 6, 24, 48, 72, 96 and 144 h) after treatment. Ki67 immunostaining and TUNEL were used to assess proliferation and apoptosis, respectively, in the jejunum and colon. Masson trichrome staining and picro-sirius red staining were used to determine the level of collagen, and immunohistochemistry was used to further assess collagen IV, fibronectin and laminin 1 and 2 expression in these tissues. Irinotecan halved cellular proliferation in the jejunum and colon at 48 and 24 h, respectively, while apoptosis peaked at 6 h ( $P < 0.05$ ). There was a substantial increase in total collagen deposits around crypts from 24 h in both regions. However, collagen IV expression decreased significantly in the crypt region in a delayed fashion ( $P < 0.05$ ). Fibronectin expression decreased significantly in jejunum and colon from 6 to 24 h following treatment ( $P < 0.05$ ). Irinotecan induced a significant alteration in epithelial cell kinetics in both the jejunum and colon, and this correlated with changes in ECM component expression. Changes in ECM expression may have a direct impact on the loss of mucosal layer integrity evident in chemotherapy-induced mucositis.

## Keywords

alimentary tract, chemotherapy, extracellular matrix components, histopathology, mucositis

In recent years, there has been increasing interest in characterizing the histopathological features of alimentary tract (AT) mucositis. In general terms, mucositis refers to the damage caused by chemotherapy or radiation therapy to mucous membranes of the AT (Sonis 2004a,b; Keefe *et al.* 2007). Different cytotoxic treatment regimens have been shown to affect different regions of the AT resulting in

region-specific toxicities, including ulceration, pain, bloating, nausea and vomiting, diarrhoea and constipation (Sonis 2004a,b; Keefe *et al.* 2007). Although these toxicities arise in a large proportion of patients receiving cytotoxic anti-cancer treatment and have detrimental effect on the treatment schedule and the patient's quality of life, an effective intervention has yet to be introduced.

Much progress has been made in understanding the molecular, cellular and tissue events that lead to the development of this condition (Sonis 2004a,b). Historically, mucositis was thought to be purely an epithelium-mediated event that occurred as a result of non-specific effects of cytotoxic anti-cancer agents (Ijiri & Potten 1983; Sonis *et al.* 2004). However, recent research has shown that development of this condition involves a multifactorial process and a cascade of events in multiple tissue structures (Sonis 2004a,b). In the gastrointestinal region, some of the main histopathological features of mucositis include the presence of degenerative enterocytes (Gibson *et al.* 2005; Logan *et al.* 2008), epithelial atrophy (Gibson *et al.* 2005), damage of submucosal vasculature (Paris *et al.* 2001), infiltration of inflammatory cells (Logan *et al.* 2008), hypersecretion of mucus (Stringer *et al.* 2009a,b,c) and increase in pathogenic bacteria (Stringer *et al.* 2008, 2009a,b,c). Other submucosal components that have been suggested to play a role in the development of mucositis are the extracellular matrix (ECM) fibrous proteins (Sonis *et al.* 2000; Sonis 2004a,b; Redding 2005).

The ECM is a complex structural network that contains fibrous proteins, proteoglycans and glycoproteins (Michael *et al.* 2003). The ECM provides structural support for the tissue. Furthermore, research in matrix biology has revealed a vital role for the ECM, in particular the fibrous proteins making up the basement membrane, in regulating epithelial cell kinetics (Yurchenco & Schittny 1990; Meredith *et al.* 1993; Beaulieu 1997). Potten *et al.* (1997) and Beaulieu (1997) have highlighted an important role for the basement membrane ECM in small intestinal and colonic crypt cell activity. Both groups demonstrated that ECM molecules are spatially expressed along the crypt-villus axis and include E-cadherin, tenascin, laminin, fibronectin, collagen IV and perlecan (Beaulieu 1997; Potten *et al.* 1997). Each of these proteins has a differential function on cell kinetics, and hence, the spatial organization of these is paramount for maintenance of mucosal layer integrity (Table 1). This spatial expression is tightly regulated by matrix metalloproteinases (MMPs) to ensure the efficient turnover of gastrointestinal tissue.

MMPs are a group of zinc-dependent endopeptidases. Although MMPs are vital for ECM homeostasis, they are regulated heavily as a result of their highly proteolytic nature. Furthermore, dysregulated production and activation of MMPs have been shown to contribute to many pathological

conditions involving excessive ECM remodelling and ultimately tissue injury (Meijer *et al.* 2007). We have shown previously an increase in MMPs in gastrointestinal tissue obtained from an animal model of irinotecan-induced mucositis (Al-Dasooqi *et al.* 2010). Although this is the case, the consequence of this increase on tissue ECM proteins has not yet been studied. Hence, the aim of this study was to characterize the change in epithelial cell kinetics and to investigate the expression of ECM proteins in the jejunum and colon following irinotecan treatment.

## Materials and methods

### Animal study

Forty-eight female dark agouti rats weighing 150–170 g were used in this study. All experimental procedures were approved by the Animal Ethics Committees of the Institute of Medical and Veterinary Sciences and the University of Adelaide and complied with the National Health and Medical Research Council (Australia) Code of Practice for Animal Care in Research and Training (2004).

Rats were randomly allocated into control ( $n = 6$ ) or experimental groups ( $n = 42$ ). Experimental group rats received 0.01 mg/kg subcutaneous atropine to reduce cholinergic reaction to irinotecan immediately prior to the administration of a single intraperitoneal dose of 200 mg/kg irinotecan, which has previously been shown to cause gastrointestinal mucositis (Gibson *et al.* 2007). Irinotecan (kindly supplied by Pfizer, Kalamazoo, USA) was administered in a sorbitol/lactic acid buffer (45 mg/ml sorbitol/0.9 mg/ml lactic acid, pH 3.4), required for activation of the drug. Rats in the control group did not receive any treatment. Rats were assessed four times daily for morbidity, body weight and diarrhoea. Diarrhoea was graded as none, mild diarrhoea (staining of anus), moderate diarrhoea (staining top of legs and lower abdomen) and severe diarrhoea (staining over legs and higher abdomen as well as continual anal leakage).

Rats were killed at various time points following irinotecan administration: 1, 6, 24, 48, 72, 96 and 144 h, by cardiac puncture and cervical dislocation under 3% isoflurane in 100% oxygen anaesthesia. The AT was dissected out from the pyloric sphincter to the rectum and flushed with chilled isotonic saline (0.9 w/v) to remove contents. A 1-cm sample of the small intestine and the colon were taken at

ECM component	Spatial expression	Effect on cell kinetics
Collagen IV	Villus	Promote migration
Fibronectin	Highest in crypts and decreasing towards tip of villus	Promote proliferation Inhibit differentiation
Laminin-1 ( $\alpha 1 \beta 1 \gamma 1$ )	Crypt-villus junction to villus tip	Promote differentiation
Laminin-2 ( $\alpha 2 \beta 1 \gamma 1$ )	Crypt	Unknown
Tenascin	Highest in villus and decreasing towards crypt	Prevent migration

ECM, extracellular matrix.

**Table 1** The role of basement membrane proteins in the regulation of cell kinetics in the gastrointestinal tract

approximately 25% and 50% of the lengths, respectively. For histological analysis, samples were fixed in 10% neutral buffered formalin, processed and embedded in paraffin.

#### *Histological assessment*

Samples of jejunum and colon were collected, processed and stained with haematoxylin and eosin as described in previous studies (Logan *et al.* 2008; Stringer *et al.* 2008, 2009a,b,c). Sections were examined by light microscopy and analysed by a professional veterinary pathologist for architectural disturbances, presence of degenerative enterocytes and inflammatory cell infiltrate.

#### *TUNEL for apoptotic cells*

Apoptosis in the jejunum and colon was determined using an *In situ* cell death detection kit (Roche Diagnostics, Indianapolis, IN, USA). Briefly, sections were cut from paraffin blocks at 44- $\mu$ m thickness and mounted onto slides. Sections were dewaxed in xylene and rehydrated through a graded series of alcohols. Sections were immersed in 0.1% TX-100 in 0.1% sodium citrate buffer for 8 min at room temperature. Following rinsing, sections were incubated with TUNEL buffer (containing Tris, 0.7 M NaCaco, CoCl<sub>2</sub>, 10% BSA in water) for 10 min at room temperature. Sections were then incubated with the reaction mixture as specified by the manufacturer's instructions. Subsequently, tissue sections were incubated with anti-fluorescein antibody (labelled with alkaline phosphatase) in a humidified chamber for 1 h. Apoptotic cells were visualized with precipitating substrate fast red in 0.1 M Tris-HCl for 15 min at room temperature. Sections were counterstained with Lillie-Mayer's haematoxylin and blued in lithium carbonate before being mounted in glycerol. Apoptotic cells were viewed by light microscopy. The number of apoptotic cells was counted in the field of view that includes five crypts.

#### *Picro-sirius red staining for collagen*

Sections were cut at 4  $\mu$ m and mounted on glass slides. The sections were dewaxed, rehydrated and stained with Weigert's haematoxylin for 10 min before washing in running tap water. Sections were then stained in picro-sirius red solution (0.5 g Sirius red F3B in 500 ml saturated aqueous picric acid solution) for 1 h. Sections were washed in two changes of acidified water solution (5 ml acetic acid in 1 l water). Finally, sections were dehydrated in three changes of 100% ethanol, cleared in xylene and mounted in a resinous medium. Sections were viewed under a light microscope. All qualitative assessments were made in a blinded fashion by one investigator (NA).

#### *Masson's trichrome staining*

Sections were cut at 4  $\mu$ m and mounted on glass slides. The sections were dewaxed, rehydrated and stained in Celestin

blue-haematoxylin before differentiating in 1% acid alcohol. Sections were washed in tap water and stained in acid fuchsin solution (0.5 g acid fuchsin and 0.5 ml glacial acetic acid in 100 ml water) for 5 min. Slides were rinsed in distilled water before being treated with phosphomolybdic acid solution (1 g phosphomolybdic acid in 100 ml water) for 5 min. Subsequently, sections were counterstained in 1% light green in acetic acid for 5 min, rinsed in distilled water and treated with 1% acetic acid for 2 min. Finally, sections were dehydrated in graded alcohols, cleared in xylene and mounted. Sections were viewed under a light microscope.

#### *Immunohistochemistry*

Control ( $n = 6$ ) and experimental ( $n = 42$ ) jejunum and colon sections were cut from paraffin blocks at 4- $\mu$ m thickness and mounted onto silane-coated slides. Sections were dewaxed in xylene and rehydrated through a graded series of alcohols. For collagen IV and Ki67 staining, sections were immersed in 10 mM citrate buffer (pH 6.0) and antigen retrieval performed by heating sections in microwave on high until boiling and on low for 10 min. Antigen retrieval for fibronectin and laminin was performed by enzymatic digestion. Endogenous peroxidase activity subsequently blocked with 3% H<sub>2</sub>O<sub>2</sub> in methanol. Non-specific antibody binding was blocked with 20% normal goat or horse serum (NHS or NGS) (Sigma, St Louis, MO, USA) in PBS for 30 min at room temperature (RT). Avidin-Biotin Blocking Kit (Vector Laboratories, Burlingame, CA, USA) was used to block endogenous avidin-biotin activity. Sections were incubated overnight with antibodies (diluted in 5% NGS or NHS) directed at collagen IV at 1:250 (Abcam, Cambridge, UK), fibronectin at 1:200 (Abcam), laminin at 1:1000 (Abcam) and Ki67 at 1:250 (Abcam) diluted in 5% NHS or NGS at 4°C. Tissue sections were incubated with the appropriate secondary antibody (20 min at RT), ABC labelling reagent (30 min at RT) and developed with DAB. Sections were counterstained with Lillie-Mayer's haematoxylin, dehydrated and cleared in xylene before being mounted. Qualitative immunohistochemistry was performed. Staining intensity was graded as follows: 0 no staining, 1 weak staining, 2 moderate staining, 3 strong staining and 4 intense staining. This qualitative staining assessment has been previously validated by published grading systems (Bowen *et al.* 2005; Yeoh *et al.* 2005; Logan *et al.* 2007) and is routinely used within our laboratory. Ki67 staining was assessed by counting stained cells per 20 crypts and averaging out to obtain the number of stained cells/crypt. All assessments were made in a blinded fashion by one investigator (NA).

#### *Statistics*

Results were statistically analysed using a Kruskal-Wallis test. *P*-value cut-offs for significance were adjusted to allow for multiple comparison according to the Stepdown Sidak procedure. Results were declared statistically significant at  $P < 0.05$ /group number.

## Results

### Response to treatment and histological analysis

As previously reported (Stringer *et al.* 2007; Logan *et al.* 2008), rats treated with irinotecan began demonstrating clinical signs of mucositis from 2 h following irinotecan administration where diarrhoea was observed in 23% of rats. The prevalence of diarrhoea peaked at 24 h where 39% of rats had mild diarrhoea and 5% had moderate diarrhoea. At 72 h, 33% of treated rats had mild diarrhoea. All diarrhoea was resolved at 144 h after irinotecan administration. None of the rats in the control groups developed diarrhoea. Irinotecan-induced death did not occur in this study (Stringer *et al.* 2007; Logan *et al.* 2008).

As reported previously, marked histological evidence of mucositis was observed in the jejunum and colon following irinotecan treatment. These changes were evident as early as 6 h following treatment and included the presence of degen-

erative enterocytes within the crypts. This was followed by more gross architectural disturbances at later time points. In the jejunum, these changes included villus blunting, epithelial atrophy and increased intensity of inflammatory cell infiltrate through mucosal tissue. Similar damage was evident in the colon at later time points with focal complete crypt ablation observed at 72 h after treatment. Tissue restitution was initiated at 144 h (Stringer *et al.* 2007; Logan *et al.* 2008).

### Proliferation and apoptosis following irinotecan

The time course of the effect of irinotecan on cell proliferation and apoptosis is shown in Figures 1 and 2, respectively. Following irinotecan, there was a significant decrease in proliferation in both the jejunum and the colon. Furthermore, the number of positively stained cells in the proliferative zones of both regions decreased significantly at 6 h following treatment (Figure 1). In the jejunal crypts, this decrease was evident between 6 and 48 h, while in the basal colon, this

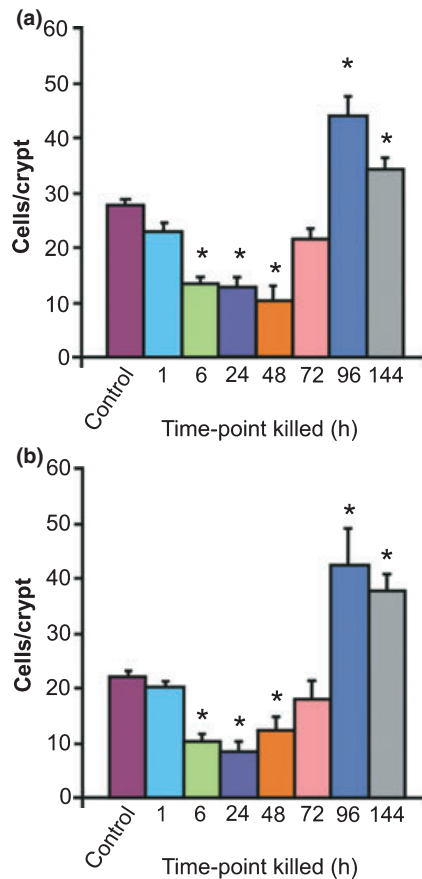


**Figure 1** Changes in cell proliferation as indicated by Ki67 immunostaining in the (a) jejunum and (b) colon at 1, 6, 24, 48, 72, 96 and 144 h following the administration of 200 mg/kg irinotecan intraperitoneally. Cells positively stained for Ki67 were counted in 20 crypts and averaged. The data are mean number of stained cells/crypt + standard error; \* $P < 0.05$  compared to untreated controls.

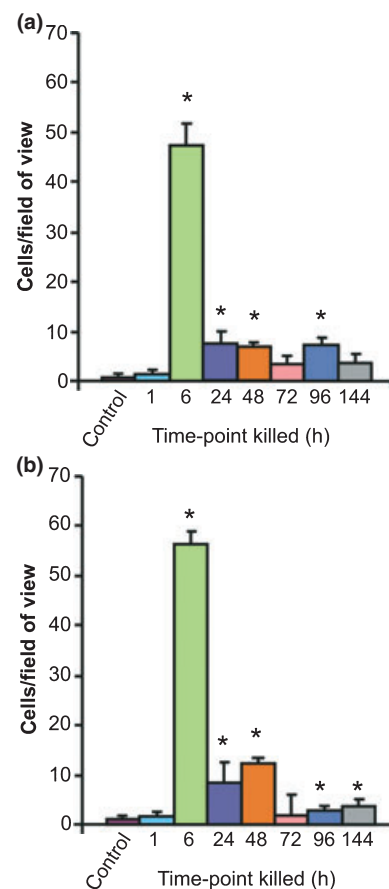


**Figure 2** Changes in cell apoptosis as identified by TUNEL assay in the (a) jejunum and (b) colon at 1, 6, 24, 48, 72, 96 and 144 h following the administration of 200 mg/kg irinotecan intraperitoneally. The data are mean number of stained cells/field of view + standard error; \* $P < 0.05$  compared to untreated controls.

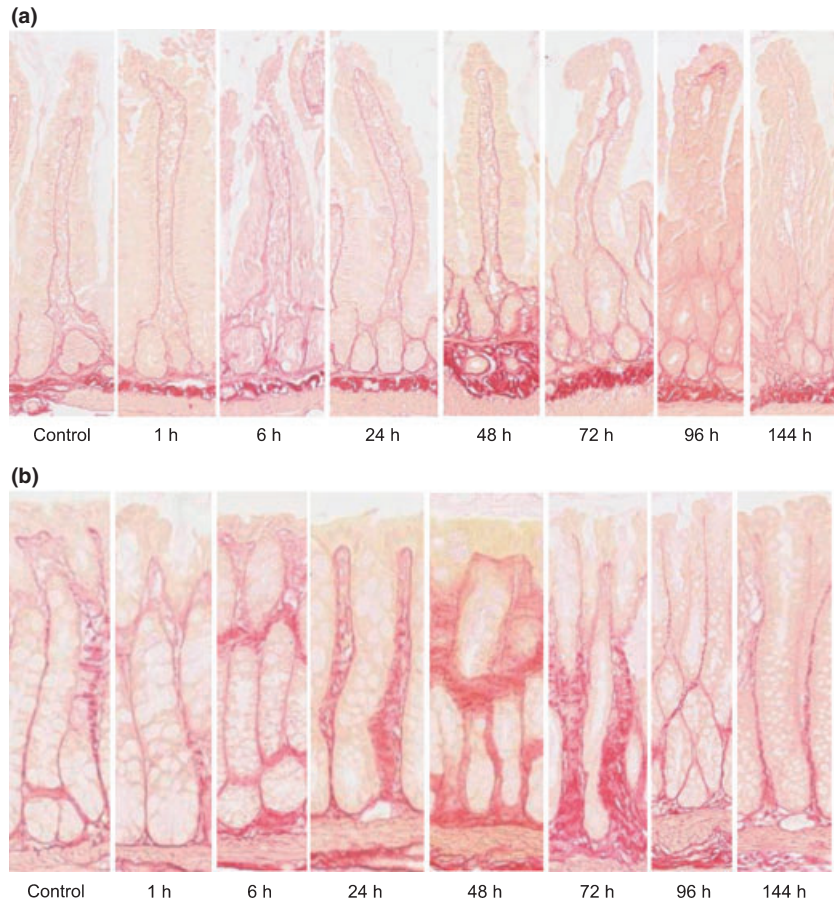


**Figure 3** Picro-sirius red staining demonstrating collagen in the (a) jejunum and (b) colon in a time course model of irinotecan-induced mucositis. Staining demonstrates collagen including the finest fibres and basement membranes, in red on a yellow background. Photomicrographs taken at 20× objective.

decrease was evident between 6 and 72 h, indicating a more profound effect of treatment on the colon. In both regions, there was a significant increase in the number of proliferative cells at 96 and 144 h above that evident in control, untreated tissue (Figure 1).

A significant change in cell apoptosis was also noted in the jejunum and colon following irinotecan administration (Figure 2). The number of stained cells in control, untreated tissue was 0.64 and 0.81 cells/five crypts in the jejunum and colon, respectively. There was a significant increase in apoptotic cell numbers at 6 h following irinotecan where 47.4 and 56.2 apoptotic cells/five crypts were observed in the jejunum and colon, respectively (Figure 2). A certain degree of recovery was indicated at 24–144 h where the number of apoptotic cells decreased, but these were still significantly elevated in comparison with control tissue (Figure 2).

#### *Collagen fibres and basement membrane collagen following irinotecan*

Picro-sirius red and Masson trichrome staining were used to illustrate collagen deposits in jejunum and colon samples (Figures 3 and 4).

**Jejunum.** In this region, control untreated tissue showed a distinct presence of collagen in the basement membrane with

moderate staining surrounding the crypts and intense staining in the submucosa (Figures 3a and 4a). From 1 to 24 h following irinotecan, a thicker, moderate staining was noted in the basement membrane underneath the villi and crypts. There was also an increase in collagen staining in the lamina propria and serosa. Between 48 and 72 h, the basement membrane underlying the crypts stained more intensely (moderate-intense), and an increase in staining was noted underneath the villi as compared to earlier time points (Figures 3a and 4a). An increase in submucosal staining was also illustrated. In the healing phase of mucositis (96–144 h), no/very weak collagen staining was observed under the epithelial layer, and a decrease in staining was noted under the crypts as compared to 48 and 72 h (Figures 3a and 4a). Submucosal, muscle and serosa staining was not altered at these later time points. Collagen staining under the crypts returned to basal level by 144 h (Figures 3a and 4a).

**Colon.** Similar expression patterns were noted for collagen in the colon. Collagen expression was uniformly moderate along the entire crypt in control, untreated tissue (Figures 3b and 4b). A gradual increase in collagen deposits was noted from 6 to 48 h after chemotherapy. At 48 h, thick collagen deposits seemed to appear in the submucosa around the base of the crypts and also along the apical region (Figures 3b

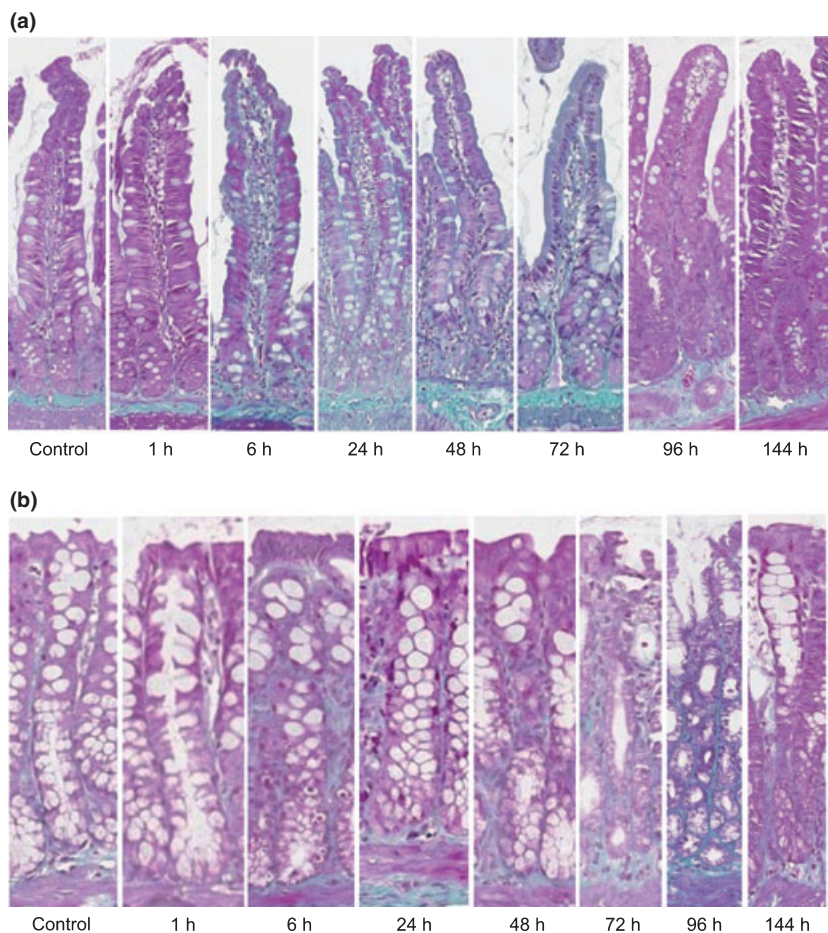


**Figure 4** Masson trichrome staining demonstrating fibrous collagen in the (a) jejunum and (b) colon in a time course model of irinotecan-induced mucositis. Fibrous collagen is stained green on a purple background. Photomicrographs taken at 20× objective.

and 4b). However, at 72 h, this thick deposit decreased in the apical region and was localized around the base of crypts. A thinning in the basement membrane underlying the apical region of the colon was also noted at this time point. Between 96 and 144 h, submucosal collagen content returned to that of untreated tissue (Figures 3b and 4b). However, a significant thinning in the basement membrane was noted in the apical region that was below the basal level expression for collagen in untreated controls (Figures 3b and 4b).

#### *The expression of ECM proteins following irinotecan*

**Jejunum.** The expression of three extracellular components was determined following irinotecan treatment. In this region, collagen IV levels decreased significantly at the later time points of 96 and 144 h following treatment in the crypts ( $P < 0.05$ ). This decrease in intensity was from moderate staining in control, untreated tissue to very weak at the later time points (Figure 5). Fibronectin expression was also investigated. In control, untreated tissue, fibronectin was expressed moderately. A decrease in expression was noted at 6–24 h following treatment in the basement membrane and submucosa underlying the villi but not the crypts, although this was not statistically significant (Figure 5). Laminin 1 and 2 levels were

also investigated; however, there was no change in expression throughout the time course (Figure 5).

**Colon.** In this region, there was no change in collagen IV or laminin 1 and 2 expression throughout the time course (Figure 6). However, fibronectin levels significantly decreased at 6 h following treatment in comparison with the untreated, control tissue ( $P < 0.05$ ). Furthermore, this change was noted in the basement membrane and submucosa underlying the basal colon only. Fibronectin expression was restored to normal from 24 h following irinotecan onwards (Figure 6).

#### **Discussion**

It has been previously demonstrated that administration of irinotecan causes gross histopathological changes throughout the AT consistent with mucositis development (Gibson *et al.* 2003; Logan *et al.* 2008). Although many morphological studies have been carried out, the changes in ECM proteins and their subsequent effect on cell kinetics have not been well characterized to date. Key findings from the present study indicate a substantial augmentation in cell kinetics, in particular cell proliferation and apoptosis, in response to irinotecan. Furthermore, this is accompanied by an increase in collagen deposits during the period of maximal damage.

**Figure 5** Extracellular matrix component staining in the jejunum. Top bars illustrate staining in villi while bottom bars illustrate staining in crypts at 1, 6, 24, 48, 72, 96 and 144 h following the administration of 200 mg/kg irinotecan intraperitoneally. All control and experimental tissue were graded by a qualitative scale. The data are means + standard error; significance indicated on the graph.

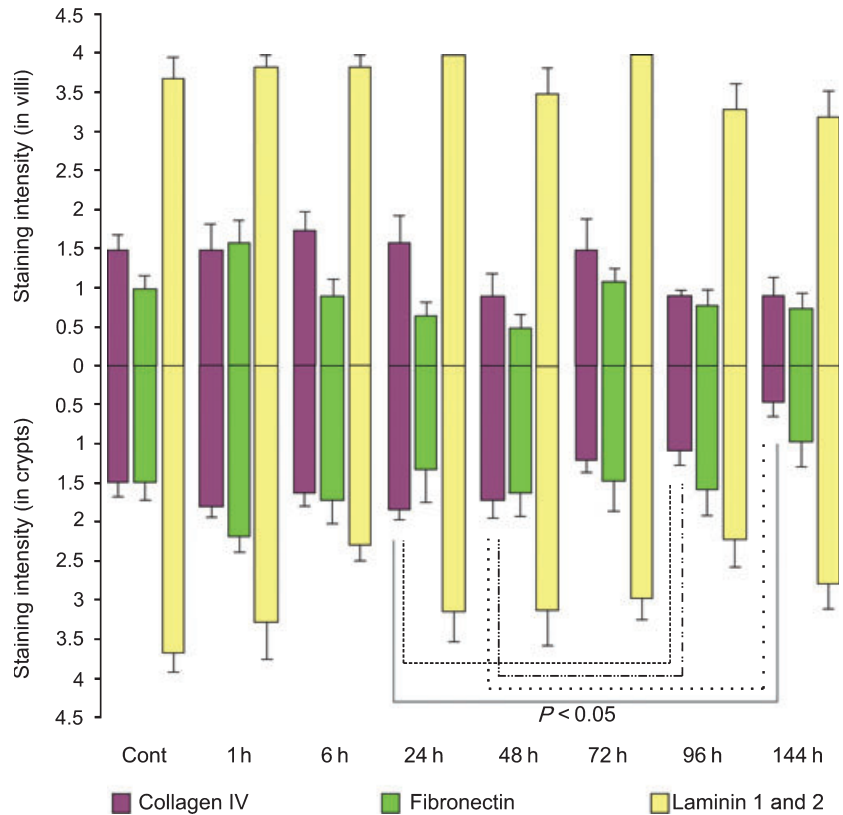
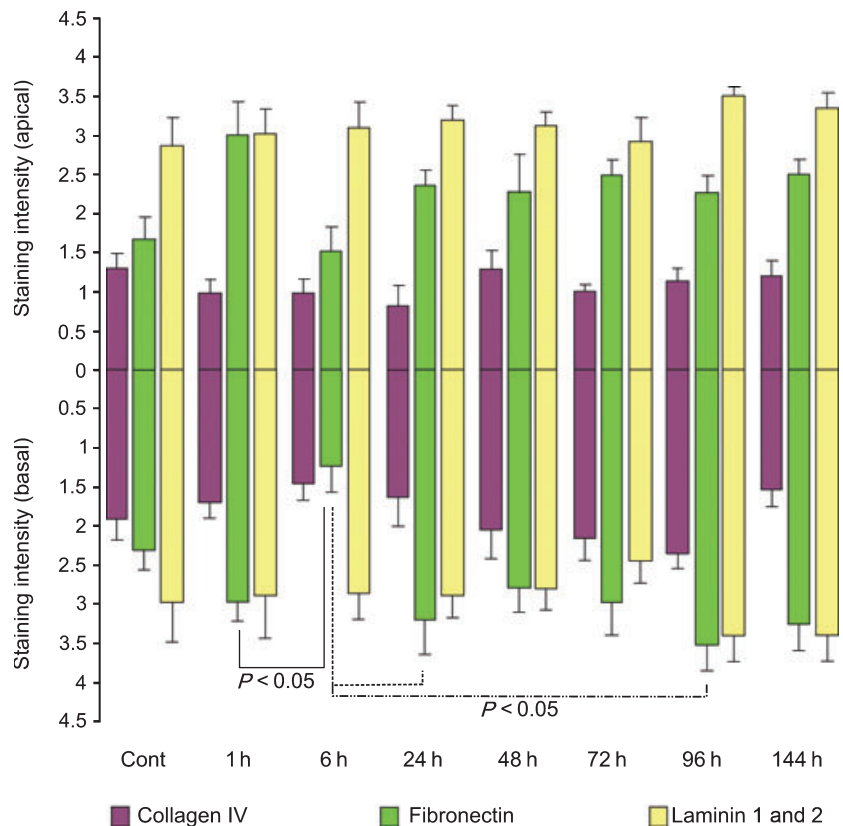


**Figure 6** Extracellular matrix component staining in the colon. Top bars illustrate staining in the apical colon while bottom bars illustrate staining in the basal colon at 1, 6, 24, 48, 72, 96 and 144 h following the administration of 200 mg/kg irinotecan intraperitoneally. All control and experimental tissue were graded by a qualitative scale. The data are means + standard error; significance indicated on the graph.



This study has also demonstrated that fibronectin may be a key player in the damage event evident following irinotecan.

The main mechanism by which chemotherapeutic drugs, such as irinotecan, induce their anti-tumour activity is by causing direct DNA damage to ultimately alter tumour cell kinetics (Ma & McLeod 2003). However, in the healthy AT, irinotecan causes mucositis by inducing both DNA as well as non-DNA damage. Through inhibiting DNA topoisomerase I, irinotecan is capable of halting DNA replication and causing DNA strand breaks resulting in altered epithelial cell kinetics. However, the majority of the initiation phase events for mucositis are because of non-DNA damage, which encompasses a cascade of biological events. Reactive oxygen species (ROS) have been shown to be a primary initiating factor for these events as a result of their broad downstream signalling (Sonis 2004a,b). Some of the signalling pathways induced by ROS are NF $\kappa$ B signalling, Wnt/ $\beta$ -catenin signalling, MAPK signalling and integrin signalling, and these affect many tissue structures, such as the ECM, hence causing tissue damage (Sonis 2004a,b).

In the AT, the ECM is vital for the maintenance of normal tissue morphology and wound healing. At the cellular level, it has been previously shown that the ability of stem cells to remain anchored at the base of the crypts or daughter cells to move away from this position results from increased or decreased affinity to ECM components (Potten *et al.* 1997). Alteration of the affinity of ECM molecules to the cell occurs through spatial changes in expression of ECM molecules or their cellular receptors. Hence, ECM components have been shown to play a key role in regulating cell behaviours, including proliferation, migration, apoptosis and differentiation. We have shown in this study that there was a significant alteration in collagen deposits in the jejunum and colon following irinotecan. Specifically, an increase in collagen deposits was noted in the basement membranes and the underlying submucosal region 48–72 h following irinotecan. This increase could serve two purposes: (1) to provide overlying tissue with sufficient structural integrity and strength especially following injury (Orberg *et al.* 1982) and (2) to allow cells to move up along the crypt-villus axis following primary tissue injury. Gibson *et al.* (2003) illustrated an increase in crypt length and a decrease in villus area 72–96 h following irinotecan administration in rats (Gibson *et al.* 2003). Furthermore, an extension in the mesenchyme has also been noted following chemotherapy treatment as indicated by Ki67 staining in this study and the work of others (Gibson *et al.* 2003; Koning *et al.* 2007). The anti-adhesive function of collagen on epithelial cell migration is well documented (Potten & Loeffler 1990; Yurchenco & Schittny 1990; Gibson *et al.* 2003; Koning *et al.* 2007). In the context of this study, an increase in collagen may play a role in the process of intestinal and colonic cell migration along the crypt axis following the injury induced by irinotecan in an attempt to repopulate the villi.

Furthermore, this study showed a decrease in collagen, specifically type IV collagen, late following irinotecan (96–

144 h). Collagen IV is a unique member of the large collagen family as it occurs only in basement membranes. In addition to providing a scaffold for assembly and mechanical stability, collagen IV is also a vital component in interaction of cells with the underlying basement membrane (Kuhn 1994). Cell culture studies have shown that collagen IV is the binding substrate for a large number of cell types (Khoshnoodi *et al.*). In the gut, collagen IV forms a three-dimensional network to provide binding sites for glycoproteins and soluble growth factors, which act as modulators of cell activity (Kuhn 1994; Groos *et al.* 2003). In the intestine, Potten *et al.* (1997) have suggested a role for collagen IV in cell migration along the villi. In the present study, we have shown that collagen IV expression decreased at 96 and 144 h following irinotecan treatment in jejunal crypts and villi. The expression of this ECM component is tightly regulated specifically by gelatinase A (MMP2). Previous research within our laboratory has demonstrated the largest increase in MMP2 tissue levels occurs during the healing phase of mucositis (i.e. 96–144 h following irinotecan treatment) (Al-Dasooqi *et al.* 2010). This is possibly caused by the anti-adhesive properties of collagen IV no longer being required for migration of cells and extension of crypts at these time points. However, even though tissues may appear normal at these later time points, it is important to note that a dysregulated structure is still present as shown here.

Another key finding in this study is the decrease in fibronectin expression noted in the jejunum as well as the colon 6–24 h following irinotecan. This is consistent with significant cell death and a decrease in proliferative activity of cells during these time points in both regions. As previously indicated by Potten *et al.* (1997), fibronectin has adhesive properties and is hence a key player in the control of proliferation and differentiation. Fibronectin carries out this role by binding to specific integrin receptors in the basement membrane in a process known as fibrillogenesis. This process encompasses the formation of specialized ECM-cell contact structures known as fibrillar adhesion points through which fibronectin-mediated signalling is initiated (Gagne *et al.* 2010). Gagne *et al.* (2010) illustrated the effects of fibronectin on cell kinetics of human intestinal epithelial cells. They concluded that the presence of this ECM component is vital for regulating migration and proliferation of these cells through activation of the PINCH-ILK-parvin (PIP) complex, which is vital for control of key regulatory cell cycle progression elements including cyclin D1, p27 and hypophosphorylated pRb (Gagne *et al.* 2010). Hence, a decrease in fibronectin expression or its receptors could deregulate the balance of proliferation and migration, hence jeopardizing mucosal integrity and the restitution of intestinal tissue following irinotecan.

In conclusion, this study has provided evidence of alteration in subepithelial components that are important in maintaining tissue structure and homeostasis. This suggests that treatment aimed at maintaining extracellular tissue compartments may be an effective intervention for irinotecan-induced intestinal injury.

## Acknowledgements

Noor Al-Dasooqi was supported by an Australian Postgraduate Award and a GlaxoSmithKline Postgraduate Support Grant; Dr Rachel J Gibson was supported by a Cancer Council Post-doctoral Fellowship and received funding from Cure Cancer and Cancer Australia; Dr Joanne M Bowen was supported by a Postdoctoral Research Fellowship from the National Health and Medical Research Council; Dr Andrea M Stringer was supported by NHMRC Postgraduate Training Scholarship; Professor Dorothy Keefe is the Cancer Council SA Chair of Cancer Medicine. Assistance with the statistical analysis for this study was provided by Mr Thomas Sullivan from the Department of Public Health, The University of Adelaide. The authors also acknowledge Ms Gail Hermanis, Discipline of Anatomy and Pathology, The University of Adelaide, for performing the histological techniques.

## References

- Al-Dasooqi N., Gibson R., Bowen J. *et al.* (2010) Matrix metalloproteinases are possible mediators for the development of alimentary tract mucositis in the DA rat. *Exp. Biol. Med.*, **235**, 1244–1256.
- Beaulieu J. (1997) Extracellular matrix components and integrins in relationship to human intestinal epithelial cell differentiation. *Prog. Histochem. Cytochem.*, **31**, 1–78.
- Bowen J., Gibson R., Keefe D., Cummins A. (2005) Cytotoxic chemotherapy up-regulates pro-apoptotic Bax and Bak in the small intestine of rats and humans. *Pathology*, **37**, 56–62.
- Gagne D., Groulx J., Benoit Y. *et al.* (2010) Integrin-linked kinase regulates migration and proliferation of human intestinal cells under a fibronectin-dependent mechanism. *J. Cell. Physiol.*, **222**, 387–400.
- Gibson R., Bowen J., Inglis M. *et al.* (2003) Irinotecan causes severe small intestinal damage, as well as colonic damage, in the rat with implanted breast cancer. *J. Gastroenterol. Hepatol.*, **18**, 1095–1100.
- Gibson R., Bowen J., Cummins A., Keefe D. (2005) Relationship between dose of methotrexate, apoptosis, p53/p21 Expression and intestinal crypt proliferation in the rat. *Clin. Exp. Med.*, **4**, 188–195.
- Gibson R., Bowen J., Alvarez E. *et al.* (2007) Establishment of a single-dose irinotecan model of gastrointestinal mucositis. *Chemotherapy*, **53**, 360–369.
- Groos S., Reale E., Hunefeld G., Luciano L. (2003) Changes in epithelial cell turnover and extracellular matrix in human small intestine after TPN. *J. Surg. Res.*, **109**, 74–85.
- Ijiri K. & Potten C. (1983) Response of intestinal cells of differing topographical and hierarchical status to ten cytotoxic drugs and five sources of radiation. *Br. J. Cancer*, **47**, 175–185.
- Keefe D., Schubert M., Elting L. *et al.* (2007) Updated clinical practice guidelines for the prevention and treatment of mucositis. *Cancer*, **109**, 820–831.
- Koning B., Lindenbergh-Kortleve D., Pieters R. *et al.* (2007) Alterations in epithelial and mesenchymal intestinal gene expression during doxorubicin-induced mucositis in mice. *Dig. Dis. Sci.*, **52**, 1814–1825.
- Kuhn K. (1994) Basement membrane (type IV) collagen. *Matrix Biol.*, **14**, 439–445.
- Logan R., Stringer A., Bowen J. *et al.* (2007) The role of pro-inflammatory cytokines in cancer treatment-induced alimentary tract mucositis: pathobiology, animal models and cytotoxic drugs. *Cancer Treat. Rev.*, **33**, 448–460.
- Logan R., Gibson R., Bowen J. *et al.* (2008) Characterisation of mucosal changes in the alimentary tract following administration of irinotecan: implications for the pathobiology of mucositis. *Cancer Chemother. Pharmacol.*, **62**, 33–41.
- Ma M. & McLeod H. (2003) Lessons learned from the irinotecan metabolic pathway. *Curr. Med. Chem.*, **10**, 41–49.
- Meijer M., Mieremet-Ooms M., Van Der Zon A. *et al.* (2007) Increased mucosal matrix metalloproteinase-1, -2, -3 and -9 activity in patients with inflammatory bowel disease and the relation with Crohn's disease phenotype. *Dig. Liver Dis.*, **39**, 733–739.
- Meredith J., Fazeli B., Schwartz M. (1993) The extracellular matrix as a cell survival factor. *Mol. Biol. Cell*, **4**, 953–961.
- Michael H., Gordon I., Wojciech P. (2003) *Histology: A Text and Atlas*. Philadelphia, PA: Lippincott Williams & Wilkins.
- Orberg J., Klein L., Hiltner A. (1982) Scanning electron microscopy of collagen fibers in intestine. *Connect. Tissue Res.*, **9**, 187–193.
- Paris F., Fuks Z., Kang A. *et al.* (2001) Endothelial apoptosis as the primary lesion initiating intestinal radiation damage in mice. *Science*, **293**, 293–297.
- Potten C. & Loeffler M. (1990) Stem cells: attributes, cycles, spirals, pitfalls and uncertainties. Lessons for and from the crypt. *Development*, **110**, 1001–1020.
- Potten C., Booth C., Pritchard D. (1997) The intestinal epithelial stem cell: the mucosal governor. *Int. J. Exp. Pathol.*, **78**, 219–243.
- Redding S. (2005) Cancer therapy-related oral mucositis. *J. Dent. Educ.*, **69**, 919–929.
- Sonis S. (2004a) A biological approach to mucositis. *J. Support Oncol*, **2**, 21–32.
- Sonis S. (2004b) The pathobiology of mucositis. *Nat. Rev. Cancer*, **4**, 277–284.
- Sonis S., Peterson R., Edwards L. *et al.* (2000) Defining mechanisms of action of interleukin-11 on the progression of radiation-induced oral mucositis in hamsters. *Oral Oncol.*, **36**, 373–381.
- Sonis S., Elting L., Keefe D. *et al.* (2004) Perspectives on cancer therapy-induced mucosal injury: pathogenesis, measurement, epidemiology, and consequences for patients. *Cancer*, **100**, 1995–2025.
- Stringer A., Gibson R., Logan R. *et al.* (2007) Chemotherapy-induced diarrhea is associated with changes in the luminal environment in the DA rat. *Exp. Biol. Med.*, **232**, 96–106.
- Stringer A., Gibson R., Logan R. *et al.* (2008) Faecal microflora and  $\beta$ -glucuronidase expression are altered in an irinotecan-induced diarrhoea model in rats. *Cancer Biol. Ther.* **7**, 1919–1925.
- Stringer A., Gibson R., Bowen J. *et al.* (2009a) Irinotecan-induced mucositis manifesting as diarrhoea corresponds with an amended intestinal flora and mucin profile. *Int. J. Exp. Pathol.*, **90**, 489–499.
- Stringer A., Gibson R., Bowen J., Keefe D. (2009b) Chemotherapy-induced changes to microflora: evidence and implications of change. *Curr. Drug Metab.*, **10**, 79–83.
- Stringer A., Gibson R., Logan R. *et al.* (2009c) Gastrointestinal microflora and mucins play a role in the development of 5-Fluorouracil-induced gastrointestinal mucositis in rats. *Exp. Biol. Med.*, **234**, 430–441.
- Yeoh A., Bowen J., Gibson R., Keefe D. (2005) Nuclear Factor  $\kappa$ B (NF $\kappa$ B) and Cyclooxygenase-2 (COX-2) expression in the irradiated colorectum is associated with subsequent histopathological changes. *Int. J. Radiat. Oncol. Biol. Phys.* **63**, 1295–1303.
- Yurchenco P. & Schittny J. (1990) Molecular architecture of basement membranes. *FASEB J.*, **4**, 1577–1590.